



**HAL**  
open science

## Tissue-selective estrogen complexes with bazedoxifene prevent metabolic dysfunction in female mice

Jun Ho Kim, Matthew S. Meyers, Saja S. Khuder, Simon L. Abdallah, Harrison T. Muturi, Lucia Russo, Chandra R. Tate, Andrea L. Hevener, Sonia M. Najjar, Corinne Amiot Leloup, et al.

► **To cite this version:**

Jun Ho Kim, Matthew S. Meyers, Saja S. Khuder, Simon L. Abdallah, Harrison T. Muturi, et al.. Tissue-selective estrogen complexes with bazedoxifene prevent metabolic dysfunction in female mice. *Molecular metabolism*, 2014, 3 (2), pp.177-190. 10.1016/j.molmet.2013.12.009 . hal-01186418

**HAL Id: hal-01186418**

**<https://hal.science/hal-01186418>**

Submitted on 24 Aug 2015

**HAL** is a multi-disciplinary open access archive for the deposit and dissemination of scientific research documents, whether they are published or not. The documents may come from teaching and research institutions in France or abroad, or from public or private research centers.

L'archive ouverte pluridisciplinaire **HAL**, est destinée au dépôt et à la diffusion de documents scientifiques de niveau recherche, publiés ou non, émanant des établissements d'enseignement et de recherche français ou étrangers, des laboratoires publics ou privés.

# Tissue-selective estrogen complexes with bazedoxifene prevent metabolic dysfunction in female mice



Jun Ho Kim<sup>1,5</sup>, Matthew S. Meyers<sup>1</sup>, Saja S. Khuder<sup>2</sup>, Simon L. Abdallah<sup>2</sup>, Harrison T. Muturi<sup>2</sup>, Lucia Russo<sup>2</sup>, Chandra R. Tate<sup>4</sup>, Andrea L. Hevener<sup>3</sup>, Sonia M. Najjar<sup>2</sup>, Corinne Leloup<sup>1,6</sup>, Franck Mauvais-Jarvis<sup>1,4,\*</sup>

## ABSTRACT

Pairing the selective estrogen receptor modulator bazedoxifene (BZA) with estrogen as a tissue-selective estrogen complex (TSEC) is a novel menopausal therapy. We investigated estrogen, BZA and TSEC effects in preventing diabetisity in ovariectomized mice during high-fat feeding. Estrogen, BZA or TSEC prevented fat accumulation in adipose tissue, liver and skeletal muscle, and improved insulin resistance and glucose intolerance without stimulating uterine growth. Estrogen, BZA and TSEC improved energy homeostasis by increasing lipid oxidation and energy expenditure, and promoted insulin action by enhancing insulin-stimulated glucose disposal and suppressing hepatic glucose production. While estrogen improved metabolic homeostasis, at least partially, by increasing hepatic production of FGF21, BZA increased hepatic expression of Sirtuin1, PPAR $\alpha$  and AMPK activity. The metabolic benefits of BZA were lost in estrogen receptor- $\alpha$  deficient mice. Thus, BZA alone or in TSEC produces metabolic signals of fasting and caloric restriction and improves energy and glucose homeostasis in female mice.

© 2014 The Authors. Published by Elsevier GmbH. Open access under CC BY-NC-ND license.

**Keywords** Tissue-selective estrogen complexes; Bazedoxifene; Menopause; Metabolic syndrome; Insulin resistance; Type 2 diabetes

## 1. INTRODUCTION

With the dramatic increase in life expectancy, many women will spend a large part of their lives in a post-menopausal state. Apart from causing degeneration of the cardiovascular, skeletal and central nervous systems [1,2], estrogen deficiency also increases risk for metabolic syndrome and type 2 diabetes [3]. Overall, the role of estrogen deficiency to the pathophysiology of chronic diseases in women is emerging as a novel therapeutic challenge that parallels the increased risk associated with conventional estrogen replacement protocols [4]. It is against this backdrop that novel therapeutic strategies targeting estrogen receptor in non-reproductive tissues may offer therapeutic benefits that reduce metabolic dysfunction associated with both ovarian failure and estrogen deficiency.

Selective estrogen receptor modulators (SERMs) are compounds that exert tissue-selective estrogen receptor (ER) agonist or antagonist activity. For example, bazedoxifene (BZA) is a novel SERM that exhibits estrogen agonist activity in bone but estrogen antagonist activity in breast and uterus [5,6]. Tissue-selective estrogen complexes (TSECs) are drugs in which a SERM and an estrogen are combined to produce mixed estrogen agonist and antagonist activity [7]. The goal of a TSEC regimen containing BZA with conjugated equine estrogens (CE) is to provide the benefits of estrogen such as reducing hot flashes and vulvar–vaginal atrophy [8–10], preventing menopausal osteoporosis [11,12] and promoting favourable effects on cardiovascular risk while simultaneously protecting the endometrium and breast from estrogen stimulation without the need for a progestin [7,13]. Current evidence

<sup>1</sup>Department of Medicine, Division of Endocrinology, Metabolism and Molecular Medicine, Northwestern University Feinberg School of Medicine, Chicago, IL 60611, USA <sup>2</sup>Center for Diabetes and Endocrine Research, Department of Physiology and Pharmacology, University of Toledo College of Medicine and Life Sciences, Toledo, OH 43614, USA <sup>3</sup>Department of Medicine, Division of Endocrinology, Diabetes and Hypertension, David Geffen School of Medicine, University of California, Los Angeles, CA, USA <sup>4</sup>Department of Medicine, Division of Endocrinology and Metabolism, Tulane University Health Sciences Center, School of Medicine, New Orleans, LA 70112, USA

<sup>5</sup>Present address: Department of Food and Biotechnology, Korea University, Sejong 339-700, South Korea

<sup>6</sup>Present address: CNRS, UMR6265, INRA, UMR1324, University of Bourgogne, CSGA, F-21000 Dijon, France

\*Corresponding author at: Division of Endocrinology and Metabolism, Tulane University Health Sciences Center, 1430 Tulane Avenue SL 53, New Orleans, LA 70112, USA. Tel.: +1 504 988 5990; fax: +1 504 988 6271. Email: fmauvais@tulane.edu (F. Mauvais-Jarvis).

**Abbreviations:** Akt, protein kinase B; AMPK $\alpha$ , AMP-activated protein kinase  $\alpha$ ; AUC, area-under the curve; BAT, brown adipose tissue; BZA, bazedoxifene; CE, conjugated equine estrogens; E2, 17 $\beta$ -estradiol; ER, estrogen receptor; FAS, fatty acid synthase; FGF21, fibroblast growth factor 21; GIR, glucose infusion rate; H&E, hematoxylin and eosin; HFD, high-fat diet; HGP, hepatic glucose production; ITT, insulin tolerance test; Lcn2, lipocalin 2; LPL, lipoprotein lipase; NAFLD, non-alcoholic fatty liver disease; OGTT, oral glucose tolerance test; OVX, ovariectomy; PTT, pyruvate tolerance test; RBP4, retinol binding protein 4; Rd, rate of whole-body glucose disappearance; RER, respiratory exchange ratio; SERM, selective estrogen receptor modulator; TBARS, thiobarbituric acid reactive substances; TG, triacylglycerol; TSEC, tissue-selective estrogen complex; UCPs, uncoupling proteins; VO<sub>2</sub>, oxygen consumption; WAT, white adipose tissue.

Received December 4, 2013 • Revision received December 20, 2013 • Accepted December 21, 2013 • Available online 9 January 2014

<http://dx.doi.org/10.1016/j.molmet.2013.12.009>

indicates that TSEC therapy consisting of the combination of CE and BZA [Duavee (TM)] [14] is an effective alternative to conventional hormone therapy for treatment of postmenopausal symptoms and prevention of osteoporosis [15,16]. However, there is currently no information on the efficacy of TSEC with BZA in preventing postmenopausal metabolic disorders. In a series of experiments that replicated postmenopausal metabolic derangements observed in older women, we investigated the effect of BZA paired with estrogens [CE or 17 $\beta$ -estradiol (E2)] on glucose and energy homeostasis in ovariectomized (OVX) mice fed a high-fat diet (HFD).

## 2. MATERIALS AND METHODS

### 2.1. Animals and surgery

Female C57BL/6J mice (Jackson Laboratory, Bar Harbor, Maine), 7 weeks of age, were housed with a 12-h light–dark cycle. After a 1-week acclimation period, mice were randomly divided into seven treatment groups as follows: (1) sham vehicle; (2) OVX+vehicle; (3) OVX+CE; (4) OVX+E2; (5) OVX+BZA; (6) OVX+CE+BZA; (7) OVX+E2+BZA. Mice were subjected to bilateral OVX or sham operation under anesthesia with 1.2% Avertin solution (i.p.). Treatment with CE, BZA, TSEC or vehicle was initiated on the day of surgery. In four separate studies, all compounds were administered orally to mice once daily for 8 weeks with vehicle (saline, 2% Tween 80, 0.5% methylcellulose), CE 2.5 mg/kg, BZA 3 mg/kg or CE 2.5 mg+BZA 3 mg/kg in saline. The dosages or concentrations of CE and BZA administered provided for the optimal maintenance of estrogen action in absence of uterine growth [11,13]. During the ovariectomy procedure, a 90-day release E2 pellet (0.5 mg/pellet, Innovation Research of America, Sarasota, FL) was implanted subcutaneously on the dorsal aspect of the neck of each animal. All mice were provided phytoestrogen-free HFD (TD04059, 52% Kcal from anhydrous milk fat, Harland Teklad, Madison, WI) and water ad libitum during the experimental period. At the end of the study (day 29 or day 57), mice were euthanized by an overdose of Avertin, and blood was collected by cardiac puncture. Mice with a null mutation of the estrogen receptor  $\alpha$  (ER $\alpha$ –/–) were generated as previously described [17]. All animal work was performed in compliance with the Institutional Animal Care and Use Committee at Northwestern University.

### 2.2. Biochemical assays

Following euthanasia, serum was separated by centrifugation at 3000g for 20 min at 4 °C and used for determination leptin, adiponectin, RBP4, Lcn2 and FGF21 using commercial ELISA kits, RBP4 (Abnova Co., Walnut, CA), Lcn2 (R&D Systems Inc., Minneapolis, MN), leptin, adiponectin and FGF21 (Millipore Co., Billerica, MA) as specified by the manufacturer. TBARS was measured in serum using a commercial kit (ZeptoMetrix Co., Buffalo, NY). For hepatic TG measurement, tissue saponification in ethanolic KOH and neutralization with MgCl<sub>2</sub> were performed as previously described [18]. Glycerol content was determined by enzymatic colorimetric methods using a commercially available kit (Sigma-Aldrich, St. Louis, MO). For the measurements of phosphorylated (T172) AMP-activated protein kinase  $\alpha$  (AMPK $\alpha$ ) in liver and muscle, total protein were extracted from liver and gastrocnemius muscle using tissue extraction reagent I (Invitrogen, Camarillo, CA). AMPK $\alpha$  [pT172] was measured by an ELISA kit (Invitrogen) as specified by the manufacturer. Insulin-stimulated Akt activity was measured in lysates from liver and muscle collected following the clamp study using

western blotting of Akt phosphorylation (S473) (Cell Signaling) and expression (Cell Signaling).

### 2.3. Histological staining

Sections of parametrial adipose tissue and liver were fixed in 10% formalin, embedded in paraffin, sectioned and stained with H&E. Adipocyte area was traced and quantified in 300 cells per mouse using ImageJ software (National Institute of Health, NIH Version v1.32j). The relative adipocyte number was calculated by dividing parametrial fat pad weight by the mean adipocyte size in each mouse ( $n=4$ /group) as described [19].

### 2.4. Studies of energy homeostasis

Food intake, locomotor activity and energy expenditure were analyzed using an indirect-calorimetric system (Labmaster, TSE Systems, Bad Homburg, Germany) in the mouse metabolic phenotyping core at Northwestern University. Mice were subjected to bilateral OVX surgery and received daily drug treatments with vehicle, CE, BZA or CE+BZA as described above for 4 weeks. Mice were then individually placed in air-tight respiratory chambers at a constant temperature (24.0  $\pm$  0.5 °C) and were acclimatized to the metabolic cages for 3 days before measurements. Energy expenditure was measured by indirect calorimetry, while locomotor activity was assessed using an infrared light beam detection system for horizontal and vertical activity. Data were collected every 30 min and averaged over the 3-day period. Energy expenditure was calculated from O<sub>2</sub> consumption and CO<sub>2</sub> production and normalized to fat-free mass. Oral drug treatments were performed at 10:00 am every day during metabolic caging.

### 2.5. Real-time fluorescent Q-PCR

Perigonadal WAT, BAT, liver and skeletal muscle tissues were homogenized in 1 mL of TRIzol reagent and then total RNA was isolated. Total RNA was reverse transcribed to cDNA using a iScript cDNA synthesis kit (Bio-Rad, Hercules, CA). cDNA was used as a template for the relative quantitation for the selected target genes with predesigned TaqMan gene expression assay kits. Each 20  $\mu$ L reaction contained 100 ng cDNA, 2  $\times$  TaqMan Fast Advanced Mastermix (Applied Biosystems, Carlsbad, CA), forward and reverse primers and TaqMan probe. All reactions were carried out in triplicate with the LightCycler<sup>®</sup> 480 II Real-Time PCR System (Roche, Mannheim, Germany) using the following conditions: 50 °C for 2 min and 95 °C for 20 s followed by 40 cycles of 95 °C for 3 s and 60 °C for 30 s. Results were expressed as a relative value after normalization to 18S rRNA.

### 2.6. FAS enzymatic activity

FAS activity was measured by the incorporation of radiolabeled malonyl-CoA into palmitate as described previously [20]. Briefly, 60–100 mg of liver tissue was homogenized in buffer (20 mM Tris, pH 7.5; 1.0 mM EDTA; 1.0 mM DTT; and phosphatase and protease inhibitors) and centrifuged at 12,000g for 30 min at 4 °C. The supernatant was incubated for 20 min at 37 °C with 166.6  $\mu$ M acetyl-CoA, 100 mM potassium phosphate (pH 6.6), 0.1  $\mu$ Ci [14C] malonyl-CoA, and 25 nM malonyl-CoA in the absence or presence of 500  $\mu$ M NADPH. The reaction was stopped with 1:1 chloroform/methanol solution, mixed for 30 min at 20 °C, and centrifuged at 12,500g for 30 min. The supernatant was vacuum-dried, and the pellet was resuspended in 200  $\mu$ L water-saturated butanol. After addition of 200  $\mu$ L ddH<sub>2</sub>O, vortexing, and spinning for 1 min, the upper layer was removed for re-extraction. The butanol layer was dried and counted. Protein was quantified by Bio-Rad

protein assay, and results were expressed as relative cpm of [<sup>14</sup>C] incorporated per microgram protein.

### 2.7. Physiological studies of glucose homeostasis

Random-fed blood glucose was measured between at 9:00 am using OneTouch Ultra 2 glucose meter (LifeScan, Inc., Milpitas, CA). For insulin levels, blood samples were collected from the tail vein in a heparinized microcapillary tube (Drummond Scientific, Broomall, PA) at week 4. Plasma insulin was measured using an ELISA kit (Millipore Co., Billerica, MA). OGTT was performed as described previously [21] with some modification. After 8-h fasting, a glucose load was administered orally (2 g/kg). For insulin tolerance test (ITT), after 6-h fasting, mice received an i.p. injection of 0.5 U/kg human insulin (Humalog, Lilly, Indianapolis, IN) in PBS. For pyruvate tolerance test (PTT), after 18-h fasting, mice received an i.p. injection of 2 g/kg sodium pyruvate (Sigma) dissolved in PBS. During OGTT, ITT and PTT, blood glucose levels were measured from the tail vein as indicated above. The measurement of insulin concentration during OGTT was done at the indicated times and as described above. The area-under the curve (AUC) was calculated for glucose and insulin for each group of animals during OGTT, ITT and PTT.

### 2.8. Euglycemic-hyperinsulinemic clamp

After 5 weeks of treatment, mice were anesthetized with 1.2% Avertin solution (i.p.), an indwelling catheter was introduced in the left jugular vein and externalized on the back 1 week before the clamp. Diet was restricted 16 h, and mice were placed in a restrainer (Briartree Scientific, MA) and underwent a euglycemic clamp with a prime continuous infusion of human insulin (Humalog, Lilly) at a rate of 24 pmol/kg/min to raise plasma insulin to 0.77 ng/mL. Glucose (15%) was infused at variable rates to maintain euglycemia. Insulin-stimulated whole-body glucose flux was estimated using a prime continuous infusion of HPLC-purified [<sup>3</sup>-<sup>3</sup>H] glucose at a 0.09  $\mu$ Ci/min throughout the clamp procedure. Blood samples (10  $\mu$ l) were collected from the tail vein for plasma [<sup>3</sup>-<sup>3</sup>H] glucose determination in 10-min intervals during the last 30 min [22]. Rates of whole-body glucose appearance (Ra) and disappearance (Rd) were calculated as the ratio of [<sup>3</sup>-<sup>3</sup>H] glucose infusion rate to the specific activity of plasma glucose during the last 30 min of the clamp. Hepatic glucose production (HGP) was determined by subtracting the glucose infusion rate (GIR) from the whole-body Ra glucose appearance [23]. Additional blood samples were collected to measure plasma insulin concentrations before and at the end of the clamp. At the end of experiment, mice were euthanized with Avertin, and tissues (WAT, liver and muscle) were rapidly removed, frozen in liquid nitrogen and stored at  $-80^{\circ}\text{C}$  for subsequent analysis.

### 2.9. Statistical analyses

Data were analyzed by one-way ANOVA using SAS software for Windows release 9.2 (SAS Institute Inc., Cary, NC, USA) on the W32\_VSHOME platform. One-way ANOVA with repeated measures was performed to assess mean differences between groups for body weight over time. To test for differences in uterine weights among the treatment groups, analysis of covariance (ANCOVA) with final body mass as covariates was used. Homogeneity of regression assumptions of the ANCOVA model were tested and met in each analysis. The Least Squares Means option using a Tukey–Kramer adjustment was used for the multiple comparisons among the treatment groups. Data are shown as the mean  $\pm$  S.E. *P* values  $< 0.05$  are statistically significant.

## 3. RESULTS

### 3.1. TSECs and BZA prevent visceral adiposity

Treatments with E2, CE and their combination as TSECs increased serum levels of E2 and estrone (E1) – the major component of CE – respectively (Suppl. Table 1). Compared to sham-operated mice, vehicle-treated OVX mice exhibited a progressive increase in body weight characterized by accumulation of intra-abdominal adipose tissue and adipocyte hypertrophy (Figure 1A–F). All estrogen treatments and BZA prevented body weight increase, visceral adipose tissue accumulation, and adipocyte hypertrophy. The combination of CE and BZA showed the greatest impact in OVX mice (Figure 1A–F). Unlike E2 and CE and as previously reported [5,6], BZA alone did not induce uterine growth (as assessed by increased tissue weight) (Figure 1G), and when combined with estrogen, BZA prevented uterine growth with a stronger effect when combined with CE (Figure 1G). All estrogen treatments suppressed WAT mRNA expression of lipoprotein lipase (LPL) (Figure 1H), an ER transcriptional target that promotes uptake of TG into adipocytes [24]. Although BZA treatment alone caused no decrease in LPL mRNA levels, it did not prevent the suppressive effect of estrogens (CE and E2) on LPL mRNA (Figure 1H). Together, the data demonstrate that whether alone or in TSEC combination, BZA exhibits estrogen mimetic action in preventing adiposity.

### 3.2. TSECs reverse abnormal serum adipokines and systemic inflammation

Metabolic dysfunction is characterized by recruitment and release of pro-inflammatory cytokines from WAT that cause insulin resistance and a general, low-grade systemic inflammatory state [25]. Serum leptin levels and the leptin/adiponectin ratio – a marker of insulin resistance and atherogenesis [26,27] – were significantly increased in vehicle-treated OVX mice relative to sham-operated mice (Table 1). Treating OVX mice with E2, CE, BZA and TSECs markedly decreased both serum leptin and the leptin/adiponectin ratio, with the strongest effect observed in mice treated with CE and CE+BZA, observations that occurred in parallel to the relative adiposity-preventive effects of these treatments. In addition, serum levels of RBP4, an adipokine that is elevated in insulin resistance and type 2 diabetes [28], were reduced in OVX mice by BZA and estrogen treatment (Table 1). However, CE and BZA, but not E2, reduced serum levels of Lcn2 (Table 1), an adipokine that is also elevated in adipose tissue and in serum of obese and insulin resistant rodents and humans [29,30]. Of note, E2 treatment increased, rather than reduced, serum Lcn2 levels, and BZA failed to reverse this E2 effect (Table 1). Nonetheless, these drugs exerted a similar effect on Lcn2 mRNA expression in both liver and WAT (data not shown). Serum levels of TBARS, a marker of oxidative stress and lipid peroxidation [31], were significantly decreased in OVX mice by E2, CE and TSEC treatments – but not by BZA alone – compared to the vehicle-treated OVX mice, thereby demonstrating that estrogens protect against lipid peroxidation and oxidative stress (Table 1). Thus, the combination of TSEC with CE improves adipose dysfunction and systemic inflammation.

### 3.3. TSECs and BZA improve hepatic and muscle lipid homeostasis

Consistent with the observation of increased non-alcoholic fatty liver disease (NAFLD) in menopause [32], vehicle-treated OVX mice exhibited diffused microvesicular fat infiltration in hepatocytes. This observation is shown by histological analysis (Figure 2A) and resulted from increased hepatic TG accumulation (Figure 2B). Both the microvesicular fat infiltration in hepatocytes and the hepatic TG accumulation were significantly reduced by all estrogen treatments (Figure 2A and B), with

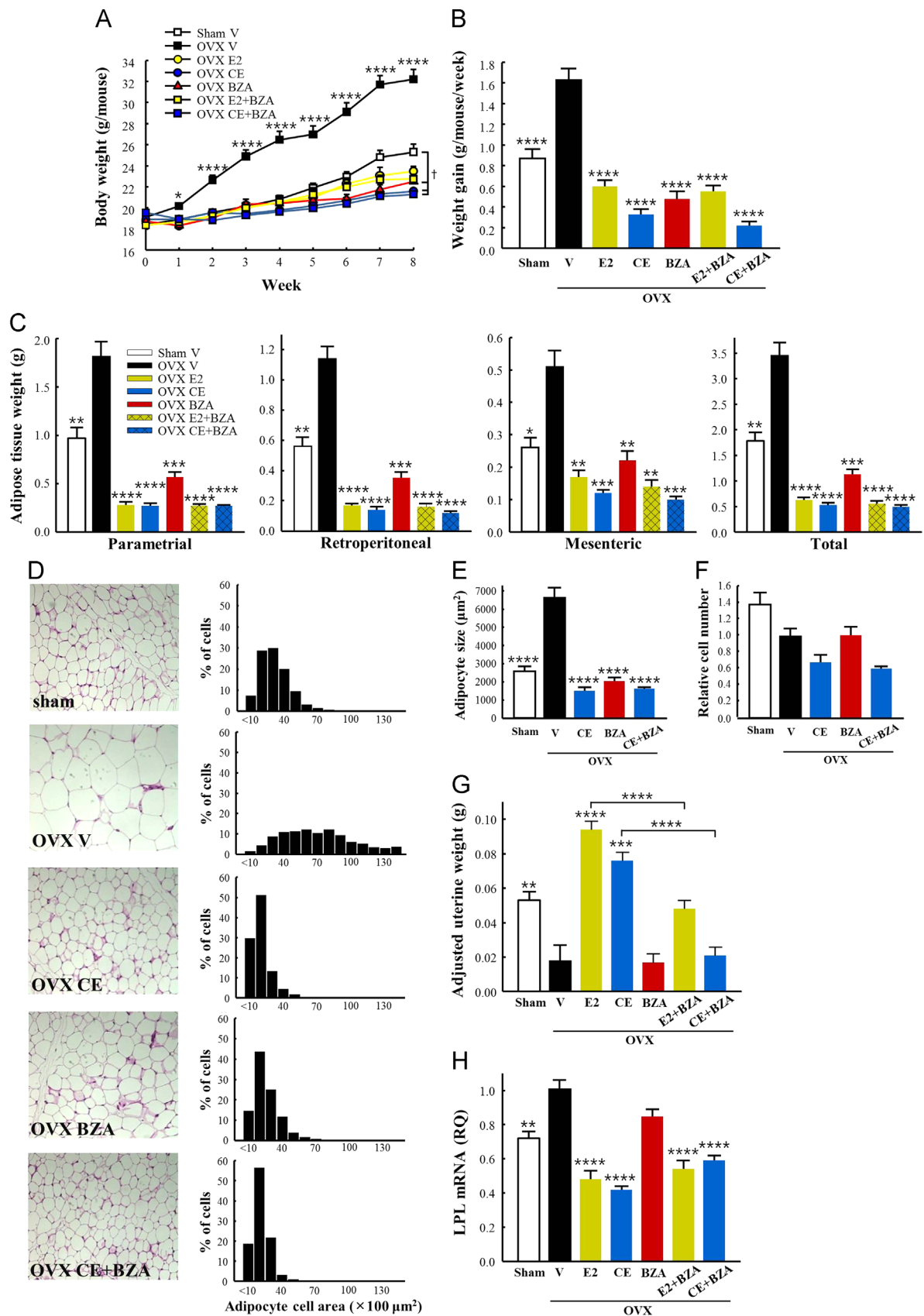


**Figure 1:** TSECs and BZA prevent visceral adiposity. Mice were subjected to sham or OVX surgeries and received the indicated drug treatments for 8 weeks. (A) Body weights, (B) weekly weight gains and (C) weights of visceral adipose depots ( $n=10$ ). (D) Representative H&E stained section of parametrial adipose tissue and distribution histogram of adipocyte size. (E) Average size of adipocytes and (F) relative adipocyte number ( $n=4$ ). (G) Uterine weights. Means are adjusted for final body mass as covariate using the ANCOVA analysis ( $n=10$ ). (H) LPL mRNA expressions from WAT ( $n=6$ ). Values represent means  $\pm$  S.E. Significantly different from all other treatment groups (A) or the OVX vehicle group (B-H) (\* $P < 0.05$ , \*\* $P < 0.01$ , \*\*\* $P < 0.001$ , \*\*\*\* $P < 0.0001$ ). †Significantly different from the sham vehicle ( $P < 0.01$ ).

	Treatment group							P
	Sham	OVX						
		Control	E2	CE	BZA	E2 + BZA	CE + BZA	
Leptin, ng/mL	18.35 ± 2.05 <sup>b</sup>	31.13 ± 2.22 <sup>a</sup>	5.69 ± 0.65 <sup>c,d</sup>	2.09 ± 0.66 <sup>d</sup>	9.47 ± 1.40 <sup>c</sup>	1.96 ± 0.61 <sup>d</sup>	1.43 ± 0.22 <sup>d</sup>	<0.0001
Adiponectin, µg/mL	14.99 ± 0.23 <sup>a</sup>	16.75 ± 1.25 <sup>a</sup>	10.40 ± 0.36 <sup>c</sup>	11.68 ± 0.29 <sup>b,c</sup>	14.05 ± 0.53 <sup>a,b</sup>	9.54 ± 0.72 <sup>c</sup>	12.02 ± 0.49 <sup>b,c</sup>	<0.0001
Leptin/adiponectin	1.23 ± 0.14 <sup>b</sup>	1.93 ± 0.18 <sup>a</sup>	0.55 ± 0.06 <sup>c,d</sup>	0.18 ± 0.06 <sup>d</sup>	0.65 ± 0.09 <sup>c</sup>	0.19 ± 0.05 <sup>d</sup>	0.12 ± 0.02 <sup>d</sup>	<0.0001
RBP4, µg/mL	4.27 ± 0.22 <sup>a,b</sup>	4.59 ± 0.12 <sup>a</sup>	3.41 ± 0.16 <sup>c,d</sup>	3.94 ± 0.26 <sup>a,b,c</sup>	3.66 ± 0.15 <sup>c,c</sup>	2.85 ± 0.16 <sup>d</sup>	3.54 ± 0.13 <sup>b,c,d</sup>	<0.0001
Lipocalin2, ng/mL	116.4 ± 13.8 <sup>b,c</sup>	112.2 ± 22.0 <sup>b,c</sup>	284.9 ± 65.1 <sup>a,b</sup>	89.8 ± 11.5 <sup>c</sup>	70.7 ± 9.6 <sup>c</sup>	348.4 ± 85.0 <sup>a</sup>	80.3 ± 14.8 <sup>c</sup>	<0.0001
TBARS, nmol MDA/mL	46.4 ± 0.8 <sup>a,b</sup>	53.6 ± 3.7 <sup>a</sup>	16.2 ± 1.2 <sup>c</sup>	37.5 ± 2.1 <sup>b</sup>	47.7 ± 3.0 <sup>a</sup>	19.4 ± 1.5 <sup>c</sup>	22.8 ± 1.0 <sup>c</sup>	<0.0001

**Table 1:** Serum adipocytokines and TBARS Mice were subjected to sham or OVX surgeries and received the daily drug treatments for 8 weeks. Values represent means ± S.E (n=10). <sup>a–d</sup>Means with different superscripts within the same row are significantly different (P < 0.05).

a more pronounced benefit associated with CE, compared to E2 treatment (P < 0.05). This difference was likely due to the oral CE delivery that exerts a hepatic first pass effect, as opposed to the transdermal application of E2 [33]. Since the Food and Drug Administration recently approved the combination of CE with BZA for treatment of vasomotor symptoms associated with menopause and prevention of postmenopausal osteoporosis [14], we continued our focus on CE for the remainder of this study.

Because estrogen is a powerful suppressor of lipogenesis [3,21], we assessed gene expression and enzymatic activity of FAS, a key enzyme in the *de novo* synthesis of fatty acids [34]. Consistent with hepatic TG content, vehicle-treated OVX mice showed higher hepatic FAS enzymatic activity (Figure 2C) that was markedly reduced by CE, BZA and TSEC treatments in a manner that paralleled their inhibitory effects on FAS mRNA levels (Figure 2D). Compared to vehicle-treated OVX mice, hepatic TBARS content paralleled its serum level in that it was significantly lower in CE and CE + BZA-treated groups, but not in those treated with BZA alone (Figure 2E).

Ectopic lipid accumulation in skeletal muscle – a well-known complication of estrogen deficiency and impaired ER $\alpha$  action – causes insulin resistance [3]. Accordingly, muscle TG content was higher in vehicle-treated OVX than vehicle-treated sham mice (Figure 2F). BZA and CE, alone or together, markedly reduced TG level in skeletal muscle of OVX mice (Figure 2F).

We next assessed phosphorylation of AMPK $\alpha$ , a major regulator of glucose and lipid metabolism in liver and skeletal muscle [35]. Compared to vehicle-treated OVX mice, AMPK $\alpha$  phosphorylation in liver was increased by BZA alone or TSEC, but not by CE alone (Figure 2G and H). This suggested that increased AMPK $\alpha$  phosphorylation by TSEC is due to BZA, but not CE. In contrast, AMPK $\alpha$  phosphorylation was not significantly altered in skeletal muscle. Thus, BZA seems to have a tissue-specific action to activate AMPK $\alpha$  selectively in liver.

#### 3.4. TSEC and BZA promote lipid oxidation and increase energy expenditure

To determine the mechanisms mediating the beneficial effects of estrogen and BZA on tissue lipid accumulation, we examined their regulation of energy homeostasis by indirect calorimetry. There were no significant differences in food intake (Suppl. Figure 1A) and total daily locomotor activity (Suppl. Figure 1B) among treatment groups. However, locomotor activity measured by vertical movements was increased by all estrogen treatments (Suppl. Figure 1C). Importantly, treatment with CE and CE + BZA significantly enhanced oxygen consumption (VO<sub>2</sub>) and increased energy expenditure compared to vehicle-treated mice (Figure 3A and B). These changes in energy balance were more pronounced with CE. In addition, BZA alone significantly increased VO<sub>2</sub>

and energy expenditure in OVX mice. All treatments produced a decrease in respiratory exchange ratio (RER), consistent with a stimulatory effect of all drugs on lipid oxidation and a preference for fat over carbohydrates as a fuel source (Figure 3C). Interestingly, a greater decrease in RER was observed in CE-treated mice, and this correlated with a larger increase in energy expenditure in this group. These data suggest that estrogen and BZA improve adiposity and ectopic lipid deposition in muscle and liver, at least in part by increasing energy expenditure via promotion of fatty acid oxidation.

#### 3.5. CE and BZA promote lipid oxidation via different pathways

To gain insight into the underlying molecular mechanisms promoting fatty acid oxidation and energy expenditure, we assessed mRNA levels of selected genes involved in the regulation of thermogenesis and cellular fuel metabolism in BAT and skeletal muscle (Suppl. Table 2). No significant alterations were detected in BAT or muscle mRNA levels of uncoupling proteins (UCPs), peroxisome proliferator-activated receptor gamma co-activator 1 $\alpha$  (PGC1 $\alpha$ ), or carnitine palmitoyltransferase 1 $\beta$ . We thus focused on the liver, a major site of lipid oxidation. Fibroblast growth factor 21 (FGF21), a hepatic hormone secreted during fasting, plays an instrumental role in inducing hepatic lipid oxidation [36]. Although OVX had no apparent effect on FGF21 hepatic mRNA and serum concentrations, treating OVX mice with E2 or CE markedly increased hepatic mRNA and serum concentrations of FGF21 (Figure 3D and E). Conversely, BZA alone or combined with CE and E2 in TSECs caused no apparent increase in hepatic FGF21 mRNA expression and serum concentrations (Figure 3D and E). To ascertain FGF21 systemic action, we next studied downstream genetic targets of FGF21. Consistent with enhanced FGF21 systemic action [37,38], mice treated with CE, E2 and TSEC – but not with BZA alone – exhibited a reduced mRNA expression of hepatic PPAR $\gamma$  and SCD-1 as well as adipose FGF21 (Suppl. Figure 2). To determine the mechanism of BZA and TSEC-induced lipid oxidation in the absence of increased hepatic production of FGF21, we next studied the expression of two master transcriptional regulators of hepatic lipid oxidation, sirtuin 1 (SIRT1) and its target, the peroxisome proliferator-activated receptor- $\alpha$  (PPAR $\alpha$ ). CE and E2 treatments had no effect on hepatic mRNA expression of either SIRT1 or PPAR $\alpha$  (Figure 3F and G). In contrast, BZA and TSECs dramatically increased hepatic mRNA expression of SIRT1 and PPAR $\alpha$ . To confirm that the increased SIRT1 expression was associated with increased SIRT1 activity, we quantified the expression of FGF15 and SHP mRNA, two genetic markers of FXR action, a target activated by SIRT1 [39]. Both FGF15 and SHP mRNA were increased by BZA but not by E2 or CE alone (Figure 3H). Further, SIRT1 normally increases the expression of genes involved in gluconeogenesis, like PEPCK by deacetylating PGC1 $\alpha$  [40]. Accordingly, PEPCK mRNA was also increased by BZA but

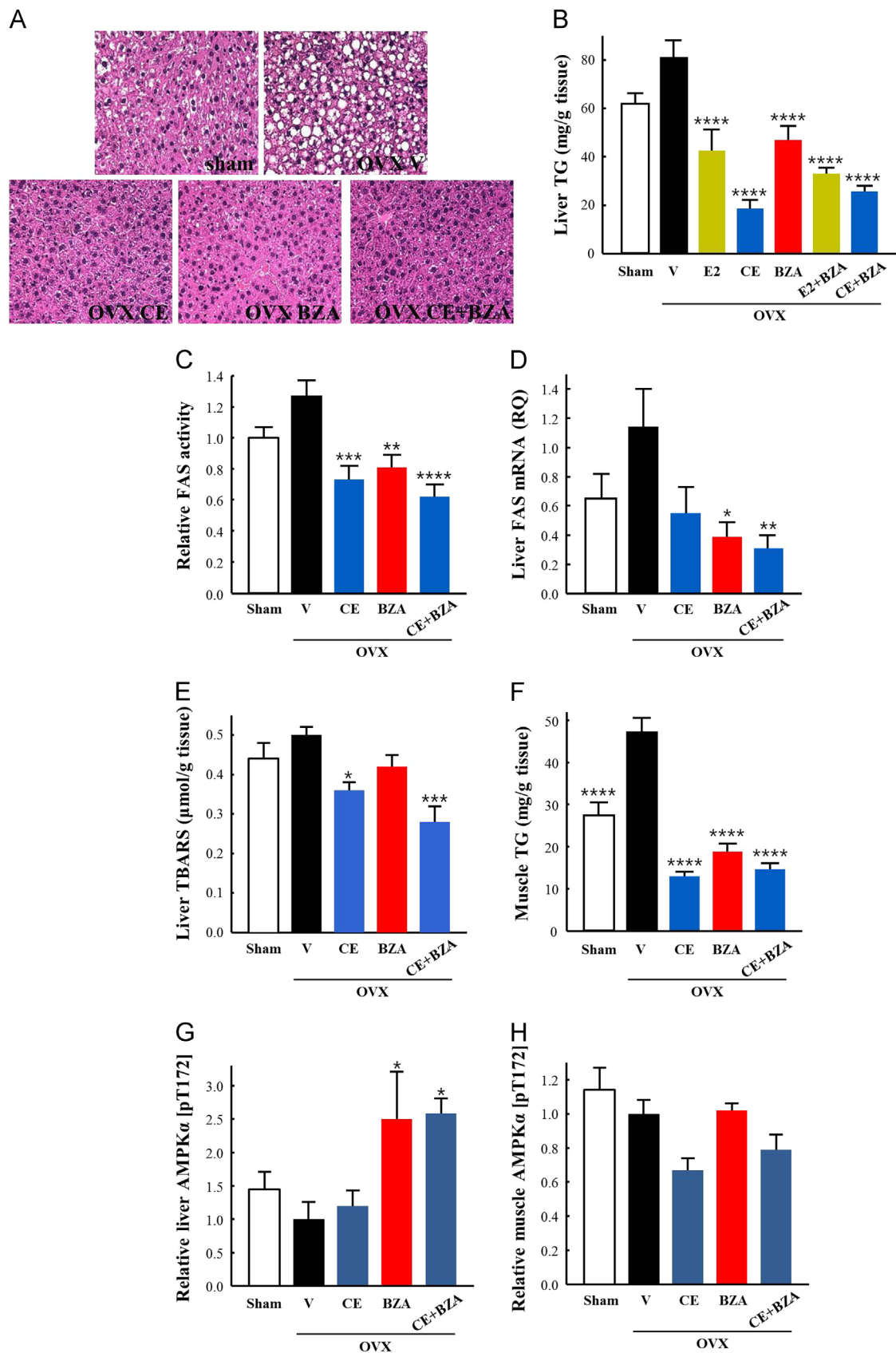


**Figure 2:** TSECs and BZA improve hepatic and muscle lipid homeostasis. Mice were subjected to sham or OVX surgeries and received the indicated drug treatments for 8 weeks. (A) Representative H&E stained sections of liver. (B) Liver TG contents ( $n=10$ ). (C) Liver FAS enzyme activity ( $n=9-12$ ). (D) Liver FAS mRNA expressions ( $n=6$ ). (E) Liver TBARS contents ( $n=6$ ). (F) Muscle TG contents ( $n=10$ ). Relative phospho-AMPK $\alpha$  (Thr 172) was quantified in (G) liver and (H) skeletal muscle ( $n=6$ ). Values represent means  $\pm$  S.E. \*Significantly different from the OVX vehicle group ( $P < 0.05$ ,  $^{**}P < 0.01$ ,  $^{***}P < 0.001$ ,  $^{****}P < 0.0001$ ).

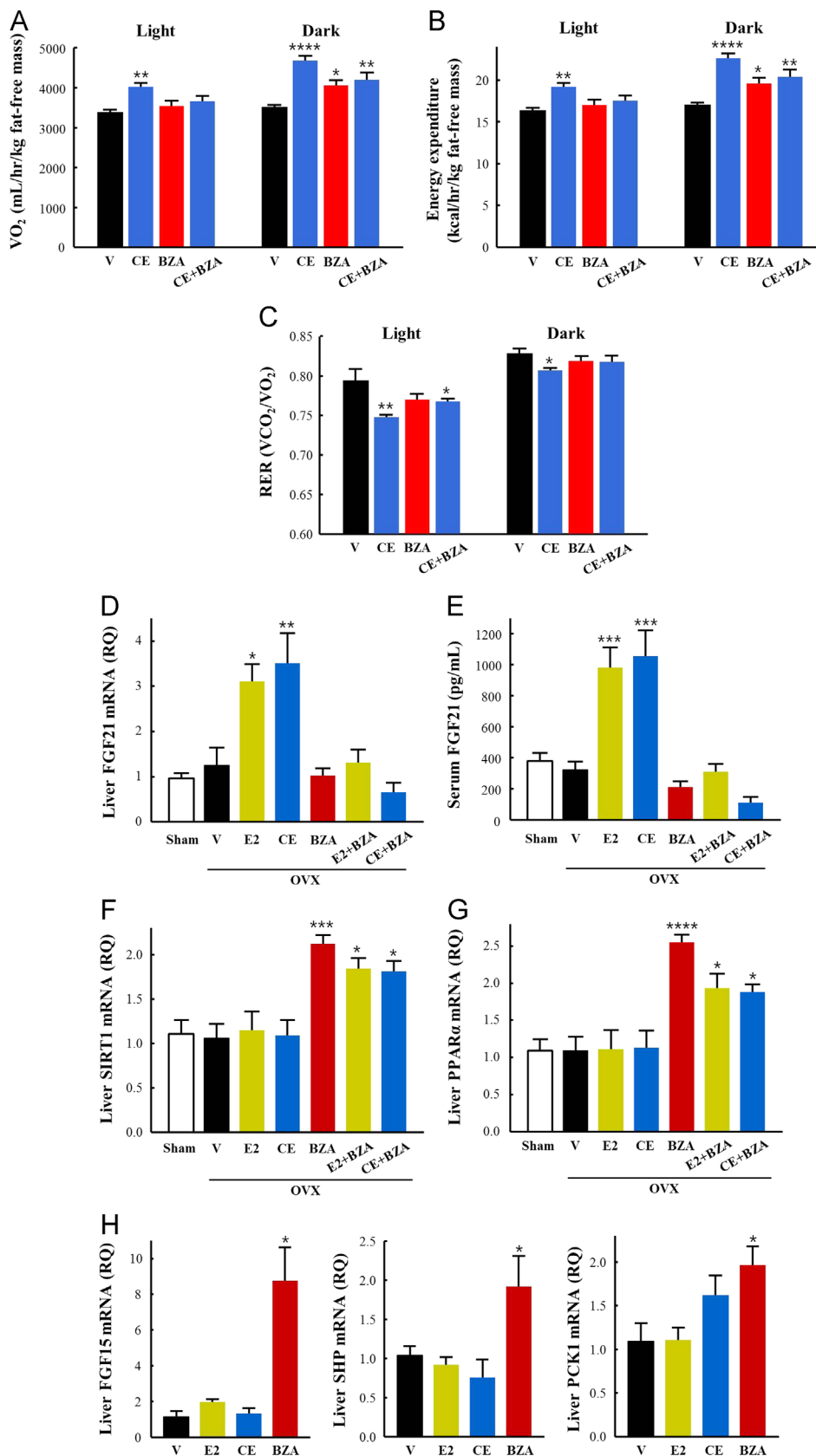


**Figure 3:** TSEC and BZA promote lipid oxidation and increase energy expenditure via different pathways. OVX mice received the indicated drug treatments for 4 weeks prior to the measurements of (A)  $O_2$  consumption, (B) energy expenditure and (C) respiratory exchange ratio ( $VCO_2/VO_2$ ) ( $n=6$ ). The  $O_2$  consumption and energy expenditure were normalized to fat-free mass. In the separate study, mice were subjected to sham or OVX surgeries and received the indicated drug treatments for 8 weeks. The following measurements were performed in the fed state (D) FGF21 mRNA, (E) serum FGF21 ( $n=10$ ), (F) SIRT1 mRNA, (G) PPAR $\alpha$  mRNA and (H) mRNAs of FGF15, SHP, and PCK1 ( $n=6$ ). mRNA were quantified by Q-PCR for liver samples. Values represent means  $\pm$  S.E. \*Significantly different from the OVX vehicle group ( $P < 0.05$ ,  $^*P < 0.01$ ,  $^{**}P < 0.001$ ,  $^{***}P < 0.0001$ ).

not by E2 or CE (Figure 3H). Together, these results demonstrate that BZA enhances SIRT1 expression and downstream hepatic actions (Figure 3H). Thus, CE and E2 activate hepatic fatty acid oxidation via FGF21 production, while BZA favors the SIRT1/PPAR $\alpha$  pathway. When estrogens and BZA are combined in TSEC, both the FGF21 and the SIRT1/PPAR $\alpha$  pathway seem to be activated.

### 3.6. TSECs and BZA improve glucose and insulin homeostasis

Except for the statistically insignificant effect of BZA on fed blood glucose levels, all drug modalities lowered fed and fasting glucose and insulin levels in OVX mice (Figure 4A–D). Moreover, all treatments improved glucose tolerance (Figure 4E and F) and decreased insulin concentrations during glucose tolerance testing (Figure 4G and H), with a statistically insignificant lowering effect of BZA on insulin concentrations (Figure 4G and H), suggesting a reversal of insulin resistance. All drug modalities, including BZA alone, enhanced glucose clearance in response to exogenous insulin during insulin tolerance testing (ITT) (Figure 4I and J). It is important to note that BZA alone improved glucose homeostasis and insulin tolerance to a similar extent as E2 and CE.

Moreover, estrogen treatments reversed adiposity (Figure 1), muscle and liver lipid accumulation (Figure 2), as well as unfavorable alterations in adipokines (Table 1) and glucose homeostasis (Figure 4) to a greater extent in OVX mice than in sham-operated mice. In fact, HFD-fed sham mice were obese and hyperglycemic compared to sham controls fed a normal chow diet (Suppl. Figure 3) and HFD-fed OVX mice treated with estrogens showed improved metabolic homeostasis to levels of controls fed a normal chow diet. This suggests that the beneficial effects of estrogens extend to both metabolic abnormalities caused by estrogen-deficiency, as well as on those caused by high fat feeding.

### 3.7. BZA improves glucose and lipid homeostasis via ER $\alpha$

Since BZA alone showed estrogen mimetic actions on metabolic parameters in OVX mice, we used global ER $\alpha$  null mice (ER $\alpha^{-/-}$ ) to investigate whether the BZA effect was dependent on ER or the result of an off-target action (Figure 5). As expected from the previous experiments, BZA protected OVX wild-type ER $\alpha^{+/+}$  mice against increased body weight, visceral fat depots, elevated serum leptin/adiponectin ratio and hepatic TG accumulation (Figure 5A–D). In contrast, BZA protection was lost in OVX ER $\alpha^{-/-}$  mice (Figure 5A–D). In addition, BZA improved glucose tolerance (Figure 5E and F) and insulin sensitivity (Figure 5G and H) in OVX wild-type mice, but failed to enhance glucose homeostasis in OVX ER $\alpha^{-/-}$  mice. These findings indicate that BZA has estrogen mimetic effects on lipid and glucose metabolism, and that these act through ER $\alpha$ .

### 3.8. TSECs but not BZA improve systemic insulin action

In order to determine whether these drugs regulate systemic insulin action, we performed euglycemic-hyperinsulinemic clamp experiments in mice treated with CE, BZA, and CE/BZA (TSEC). During the clamp, plasma insulin levels were raised but remained at physiological levels that were statistically indistinguishable among treatment groups (Suppl. Table 3). Compared to vehicle-treated mice, at steady state insulin levels, the glucose infusion rate (GIR) was significantly elevated in OVX mice treated with CE, TSEC, and to a lesser extent, with BZA (Figure 6A), indicating a lower effect of BZA on systemic insulin resistance. GIR was not significantly different between BZA and vehicle-treated mice (Figure 6A). Insulin-stimulated whole body glucose flux (Rd) was increased in mice treated with CE and TSEC compared to vehicle, while the modest increase in Rd in BZA-treated mice did not reach

statistical significance (Figure 6B). These observations suggest a modest increase in overall glucose turnover with BZA compared to CE and TSEC. Both CE and TSEC, but not BZA, enhanced the ability of insulin to suppress hepatic glucose production (HGP) (Figure 6C). To further explore the impact of estrogens on liver glucose metabolism, we examined pyruvate incorporation into glucose via gluconeogenesis in a pyruvate tolerance test (PTT) (Figure 6D and E). Mice treated with estrogen exhibited lower glucose levels than vehicle-treated OVX mice, as reflected by the area under the curve (AUC). In contrast, glucose levels in BZA-treated mice were similar to those observed in vehicle-treated OVX mice. These data indicate that CE and TSEC reduce hepatic glucose output during pyruvate challenge, presumably via suppressing gluconeogenesis. Taken together, these results demonstrate that CE and TSEC improve systemic insulin response by enhancing insulin suppression of HGP and glucose uptake in peripheral tissues. The effect of these drugs on Rd and HGP could be at least partly mediated by increased insulin-stimulated Akt phosphorylation in skeletal muscle and liver, respectively, as suggested by tissues isolated from clamped mice (Figure 6F and G).

Because the carcinoembryonic antigen-related cell adhesion molecule (CEACAM1) reduces liver FAS activity when phosphorylated by insulin [20], we then examined the effect of these drugs on CEACAM1 expression and phosphorylation in liver. OVX produced a minor reduction in Ceacam1 mRNA in vehicle-treated mice (Figure 6H). Relative to vehicle-treated OVX mice, CE, TSEC and BZA induced hepatic Ceacam1 mRNA levels (Figure 6H). This translated into an increase in CEACAM1 protein expression and phosphorylation levels in livers derived from pre-treated OVX mice that had undergone a hyperinsulinemic-euglycemic clamp (Figure 6I).

## 4. DISCUSSION

Prevention of adiposity by estrogen is mediated primarily by ER $\alpha$ -dependent mechanisms in the periphery as well as in the central nervous system [3]. Similar to the effect of estrogen, this study shows that the anti-adiposity effects of BZA are abolished in ER $\alpha$ -deficient mice, thereby demonstrating that BZA-associated metabolic actions are also ER $\alpha$ -dependent. However, the relative contributions of peripheral, versus central actions of ER $\alpha$  in preventing adiposity during CE therapy remain unknown. We observe that oral administration of CE and BZA in estrogen-deficient OVX mice increases lipid oxidation, oxygen consumption and energy expenditure without significantly altering food intake or overall locomotor activity, and importantly, without increasing BAT-mediated thermogenesis (based on unaltered mRNA levels of genetic markers in BAT). These findings are consistent with a recent study showing that although both subcutaneous and intra-cerebroventricular administration of E2 increase oxygen consumption and energy expenditure in OVX mice, only central E2 administration elevates locomotor activity, body temperature, and expression of thermogenic markers in BAT [41]. This suggests that oral administration of CE, BZA, and TSEC enhances energy expenditure and prevents adiposity in estrogen-deficient OVX mice independently of central stimulation of sympathetic outflow to BAT by ER $\alpha$ . In support of this notion, little circulating estrone sulfate is available to the brain following an oral CE administration [42], and BZA has not been shown to cross the blood brain barrier [43]. Thus, it is likely that peripherally administered CE and E2 increase lipid oxidation and energy expenditure largely by engaging peripheral ER actions, thus increasing basal metabolic rate. Two non-exclusive mechanisms could mediate this effect. The first involves induction of

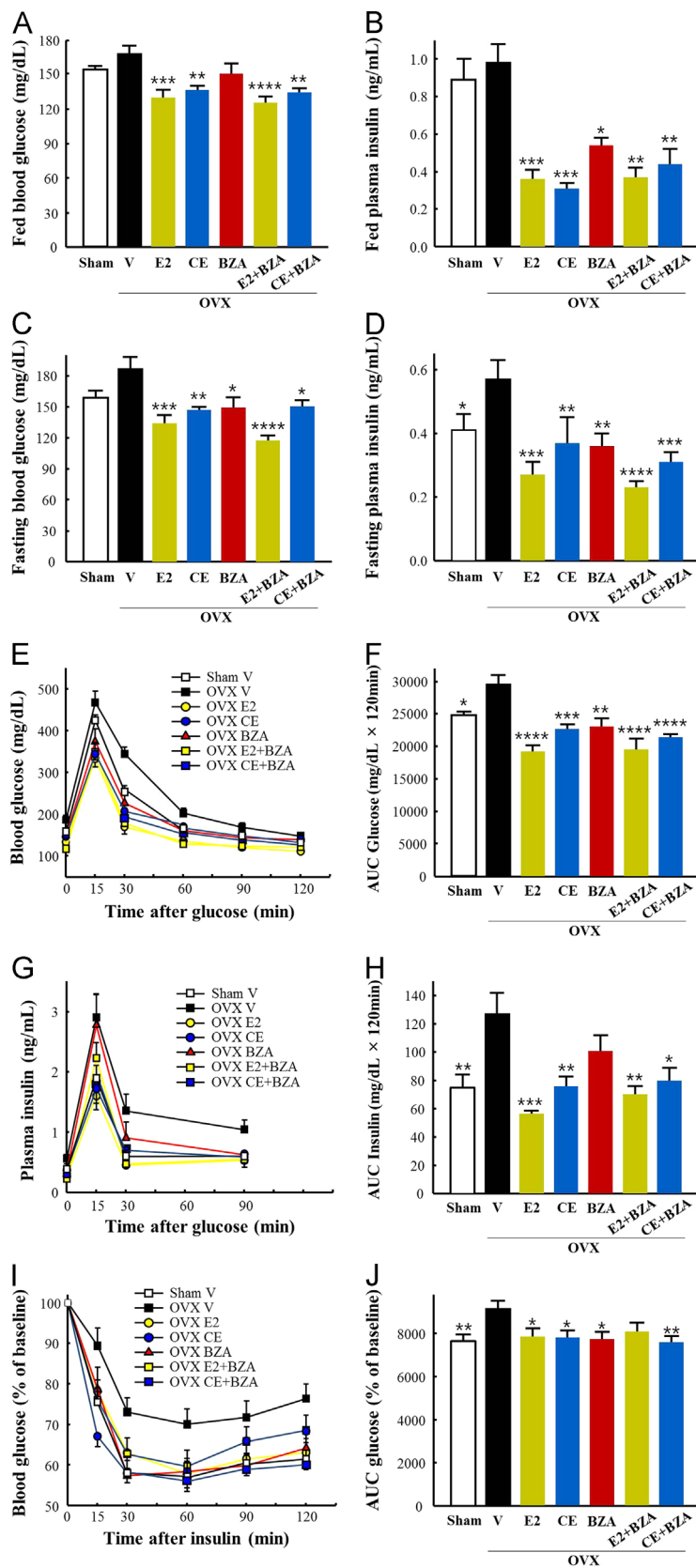


**Figure 4:** TSECs and BZA improve glucose and insulin homeostasis. Mice were subjected to sham or OVX surgeries and received the indicated drug treatments for 4 weeks prior to the measurements of (A) fed blood glucose, (B) fed plasma insulin, (C) 8-h fasting blood glucose, (D) 8-h fasting plasma insulin, (E) glucose concentrations during OGTT, (F) area under the curve (AUC) for glucose for (E), (G) insulin concentrations during OGTT and (H) AUC for insulin for (G), (I), Glucose concentrations during the ITT (Week 7) and (J) AUC for glucose during ITT. Values represent means  $\pm$  S.E. ( $n=10$ ). \*Significantly different from the OVX vehicle group ( $P < 0.05$ ,  $P < 0.01$ ,  $P < 0.001$ ,  $P < 0.0001$ ).

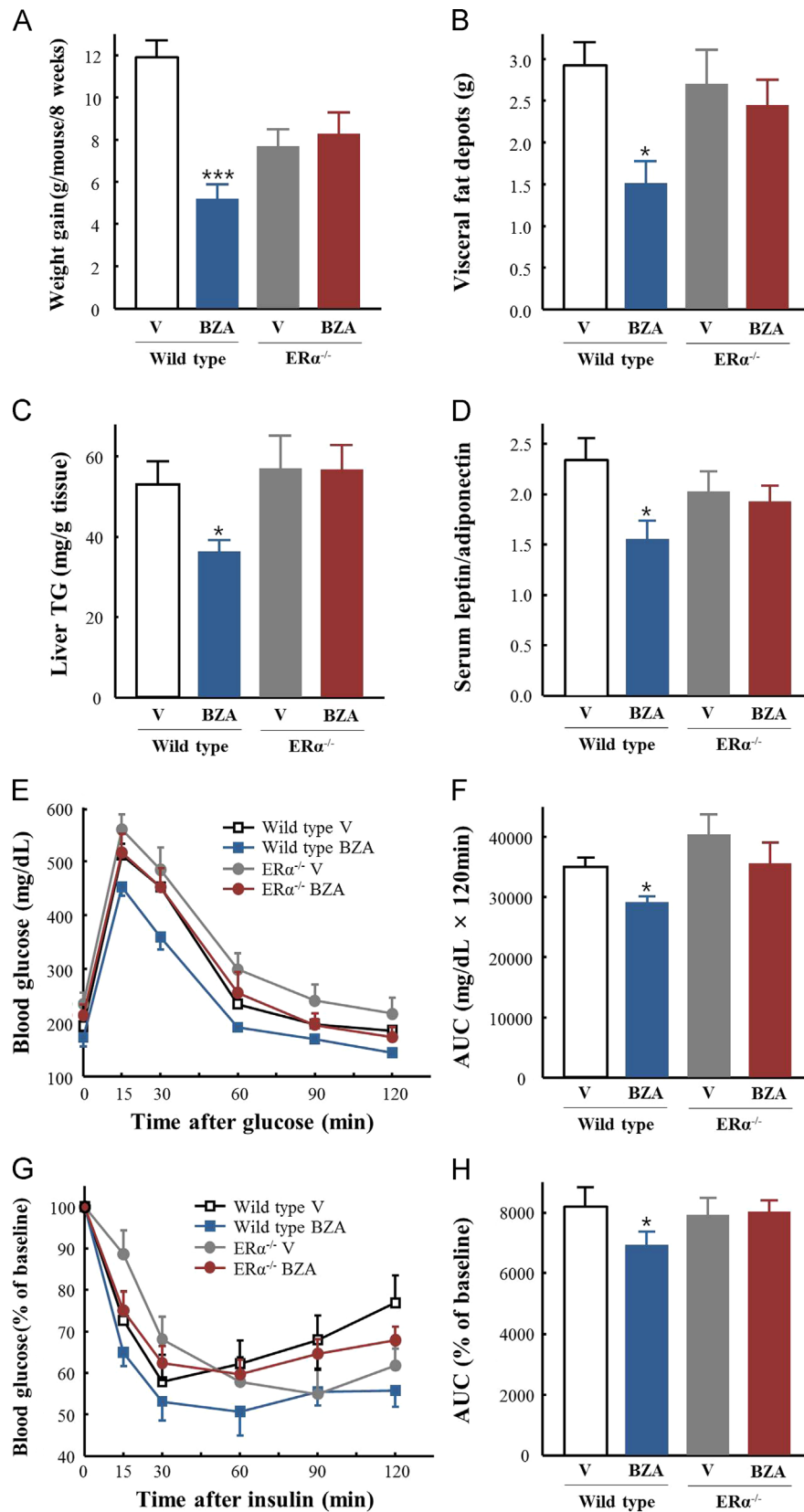


**Figure 5:** BZA improves glucose and lipid homeostasis via ER $\alpha$ . Mice were subjected to OVX surgery and received the indicated drug treatments for 8 weeks. (A) Weight gain, (B) visceral fat depot weights, (C) hepatic TG content, (D) serum leptin/adiponectin ratio. (E) Glucose concentrations during OGTT and (F) area under the curve (AUC) for glucose at Week 4. (G) Glucose concentrations during the ITT and (H) AUC for glucose at Week 7. Values represent means  $\pm$  S.E. ( $n=6$ ). \*Significantly different from the corresponding vehicle groups ( $P < 0.05$ , \*\* $P < 0.01$ , \*\*\* $P < 0.001$ , \*\*\*\* $P < 0.0001$ ).

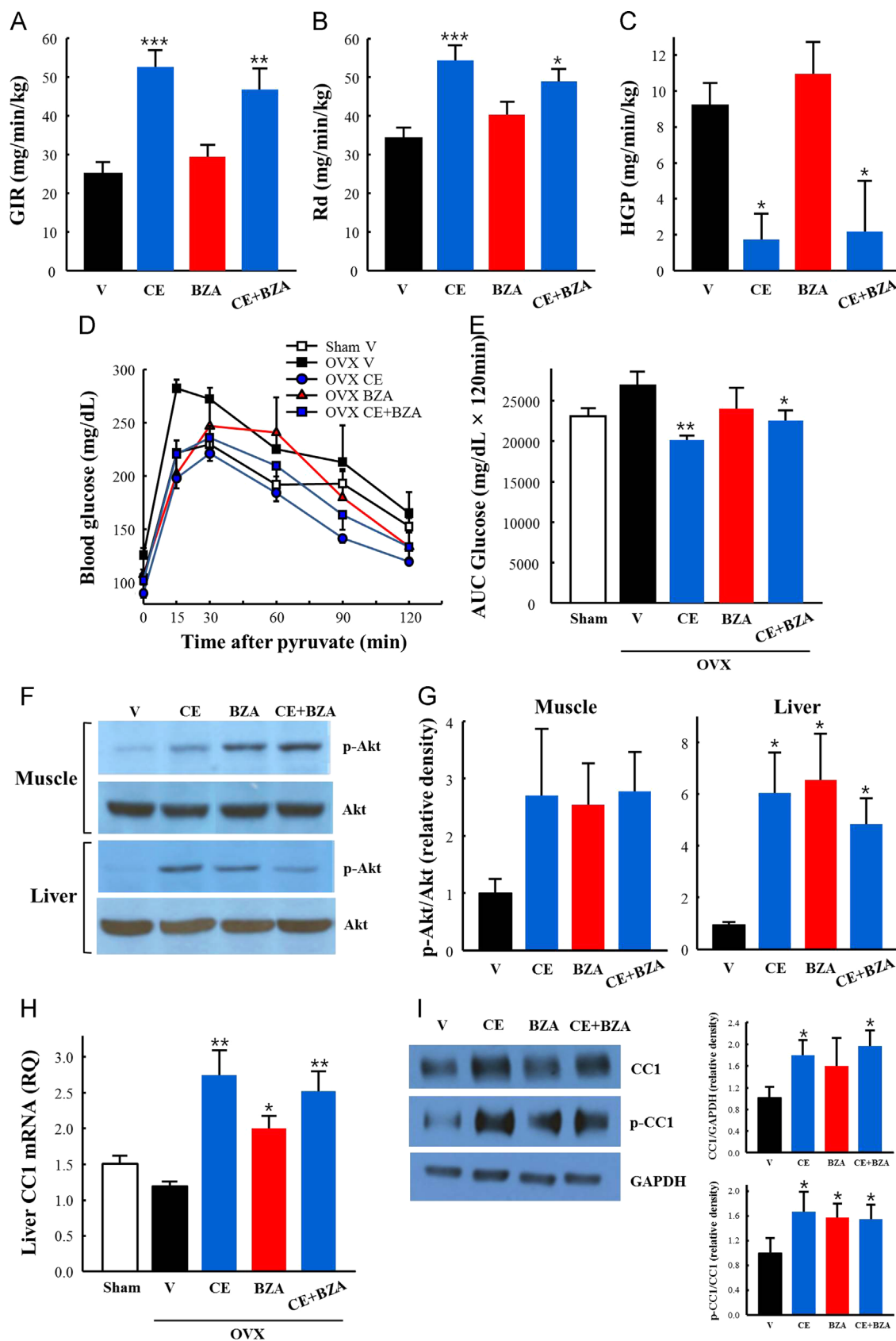


**Figure 6:** CE and TSEC improve systemic insulin action. The OVX mice received the indicated drug treatments for 4 weeks and subjected to a euglycemic-hyperinsulinemic clamp for measurement of (A) GIR, (B) Rd and (C) insulin suppression of HGP ( $n=6-9$ ). In the separate study, (D) glucose concentrations were measured during a PTT performed at Week 4; (E) AUC for glucose during PTT ( $n=6$ ). (F) Insulin-stimulated Akt activity was measured in lysates from liver and muscle collected following the clamp study using western blotting of Akt phosphorylation and expression. (G) Quantification of immunoblot is shown. p-Akt, phosphorylated-Akt; Akt, total Akt (muscle,  $n=3$ ; liver,  $n=4$ ). In the separate study, sham or OVX mice received the indicated drug treatments for 8 weeks prior to the measurements of (H) hepatic CC1 mRNA expressions ( $n=6$ ). (I) CEACAM1 expression (CC1) and phosphorylation (pCC1) were measured by Western blotting using lysates from liver collected following the clamp study ( $n=4$ ). Values represent means  $\pm$  S.E. \*Significantly different from the OVX vehicle group ( $P < 0.05$ ,  $P < 0.01$ ,  $P < 0.001$ ).

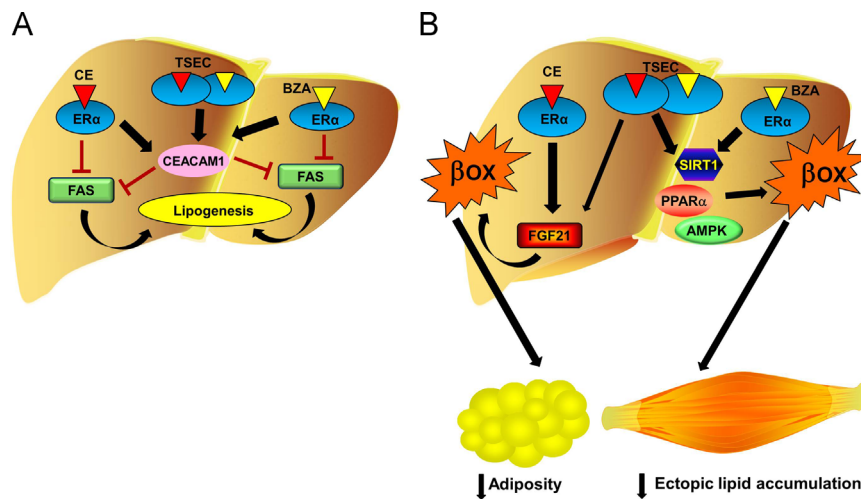


**Figure 7:** Proposed mechanism of estrogen, BZA and TSEC effects of hepatic lipid metabolism. (A) Estrogen (CE and E2), TSEC and BZA all induce CEACAM1 expression and phosphorylation thus inhibiting FAS activity and preventing hepatic lipogenesis. (B) CE and E2 promote hepatic lipid oxidation through FGF21 production, thereby elevating basal metabolic rate. In contrast, BZA promotes hepatic lipid oxidation by increasing SIRT1 and PPAR $\alpha$  expression as well as increasing AMPK activity. The combination of estrogen and BZA in a TSEC promotes a state of increased FGF21 production and sensitivity. Altogether, these effects promote lipid combustion in liver that prevents fat storage in skeletal muscle and adipose tissue.

hepatic production and release of the hormone FGF21 during the fed state. Treatment with E2 or CE similarly elevates serum FGF21 concentrations to levels normally observed in fasted mice, resulting in enhanced lipid oxidation and metabolic rate [37,38]. In contrast, BZA does not increase hepatic production of FGF21. Instead, BZA alone or in TSEC increases hepatic expression and activity of SIRT1, PPAR $\alpha$  as well as hepatic AMPK activity, all known metabolic switches of the fasting state that promote hepatic lipid oxidation [44–46]. This combined metabolic switch probably accounts for the retained stimulatory effect of BZA on lipid oxidation and energy expenditure in the absence of FGF21 release. This may also explain why CE and E2 combined with BZA increase systemic markers of FGF21 action without apparent increase in hepatic FGF21 mRNA expression and serum concentrations. We propose that BZA, by increasing hepatic expression and activity of SIRT1 and PPAR $\alpha$ , sensitizes to FGF21 action thus explaining why FGF21 mRNA and circulating concentrations remain normal despite enhanced production. Thus, the combination of estrogen and BZA in a TSEC promotes a state of increased FGF21 production and sensitivity without increase in FGF21 circulating concentrations.

Secondly, E2 and CE could increase  $\beta$ -oxidation through direct ER $\alpha$  action in skeletal muscle. Muscle-specific and global ER $\alpha$  null deletions severely impair fatty acid  $\beta$ -oxidation and cause accumulation of bioactive lipids in muscle [3,47,48]. Accordingly, the current study shows that CE and BZA improve ectopic lipid accumulation in skeletal muscle.

Like CE, BZA reduces FAS expression and activity in association with a decrease in lipid accumulation in liver. This appears to be mediated in part by inducing CEACAM1 expression and insulin-stimulated phosphorylation, which triggers CEACAM1 binding to and downregulation of FAS activity [20]. It is unclear whether ER activation by CE and BZA induces CEACAM1 transcription, or if these drugs induce CEACAM1 by enhancing insulin signaling, which in turn, activates the transcription of Ceacam1 gene [49]. Of note, the suppression of FAS expression could also be mediated by ER $\alpha$  suppression of SREBP1c maturation [50,51].

Taken together, these findings suggest that the anti-obesity effect of CE, BZA and TSEC in HFD-fed OVX mice result from a combined inhibition of lipogenesis and stimulation of lipid oxidation. CE, TSEC and BZA all induce CEACAM1 and inhibit FAS thus preventing hepatic lipogenesis. However, CE and E2 promote hepatic lipid oxidation at least partially

through FGF21 production, thereby elevating basal metabolic rate. In contrast, BZA and TSEC promote hepatic lipid oxidation via a SIRT1/PPAR $\alpha$  and AMPK pathway. Altogether, this promotes lipid combustion in liver that prevents fat storage in skeletal muscle and adipose tissue. Figure 7 summarizes the proposed mechanisms of estrogens and BZA hepatic action on lipid homeostasis. It should be emphasized, however, that further studies are needed to study the effect of estrogen on white fat “browning”, in which certain WAT depots significantly acquire the thermogenic, fat-burning properties of BAT. Further, even though our data suggest that peripherally administered CE and E2 prevents adipose accumulation mainly via peripheral ER action, further studies using tissue-specific ER $\alpha$  null mice are needed to distinguish ER $\alpha$ -dependent pathways mediating central versus peripheral regulatory effects of CE and BZA on metabolism.

Estrogen promotes insulin-stimulated glucose uptake in skeletal muscle and enhances insulin suppression of hepatic glucose production mainly through ER $\alpha$  action [48,52–55]. These experiments also show that CE enhances muscle and liver insulin action during clamp conditions and importantly, BZA does not antagonize the effect of estrogens on glucose homeostasis and insulin sensitivity when combined in a TSEC. In fact, BZA alone improves insulin sensitivity and glucose tolerance in wild-type, but not ER $\alpha$  null mice, demonstrating that the insulin sensitizing action of BZA is likely mediated by ER $\alpha$ . Furthermore, BZA enhances the ability of insulin to clear glucose during an insulin tolerance test. This likely results from the observed enhanced insulin-stimulated Akt signaling and improved insulin-mediated glucose disposal in skeletal muscle. Indeed, we observe a mild positive effect of BZA on glucose turnover (Rd) in the absence of an effect on insulin suppression of hepatic glucose production and on pyruvate incorporation into glucose. Thus, BZA-induced improvement in glucose clearance in response to insulin is probably due to enhanced insulin action via ER $\alpha$ -dependent pathways in skeletal muscle. Further studies employing hepatocyte- and muscle-specific conditional ER $\alpha$  knockout mice are needed to identify the mechanisms underlying the metabolic regulatory effect of BZA.

Several lines of evidence suggest a close relationship between Lcn2 and estrogens. Lcn2 is a putative target gene of estrogens, and Lcn2 deficiency results in decreased estrogen production and action [56]. Interestingly, E2, but not CE, increases circulating levels of Lcn2 and its

expression in white adipose tissue, but BZA did not reverse E2-induced production of Lcn2. Lcn2 promotes breast cancer progression by inducing mesenchymal transition through ER $\alpha$  [57], and its over-expression increases cell migration, invasion, and lung metastasis in murine breast cancer cells [58]. Although this study did not compare the efficacy of CE to transdermal E2 in breast cancer treatment, our results suggest that oral CE (in combination with BZA) may offer a safer approach than E2 to decrease the risk of breast cancer, at least partly, by suppressing Lcn2-mediated cancer progression.

In conclusion, our data demonstrate that BZA exhibits estrogen-mimetic action with regard to glucose and energy homeostasis. More importantly, they also show that TSECs that combine CE or E2 with BZA prevent estrogen deficiency-induced visceral adiposity, systemic inflammation, insulin resistance, and glucose intolerance as efficiently as CE or E2 alone, and importantly, without causing endometrial hyperplasia. These observations provide novel insights into the mechanisms underlying the beneficial effects of TSEC containing BZA with estrogens in reversing postmenopausal metabolic abnormalities, and suggest that clinical studies in postmenopausal women are warranted.

## ACKNOWLEDGMENTS

We thank the mouse metabolic phenotyping core at Northwestern University Feinberg School of Medicine for calorimetric studies. This study was funded by an investigator initiated grant from Pfizer, Inc to FMJ, the National Institutes of Health R01 DK074970 to FMJ, the American Heart Association (11IRG5570010) to FMJ and the National Institutes of Health (R01 DK054254, R01 DK083850 and R01 HL112248) to SMN.

## CONFLICT OF INTEREST

Dr. Mauvais-Jarvis received research funding from Pfizer, Inc. However, Pfizer had no involvement in the study design, the collection, analysis and interpretation of data. Pfizer had no involvement in the writing of the report and no involvement in the decision to submit the article for publication. The other authors have no conflict of interest.

## APPENDIX A. SUPPORTING INFORMATION

Supplementary data associated with this article can be found in the online version at <http://dx.doi.org/10.1016/j.molmet.2013.12.009>.

## REFERENCES

- [1] Carr, M.C., 2003. The emergence of the metabolic syndrome with menopause. *Journal of Clinical Endocrinology and Metabolism* 88 (6):2404–2411.
- [2] Mauvais-Jarvis, F., 2011. Estrogen and androgen receptors: regulators of fuel homeostasis and emerging targets for diabetes and obesity. *Trends in Endocrinology and Metabolism* 22 (1):24–33.
- [3] Mauvais-Jarvis, F., Clegg, D.J., Hevener, A.L., 2013. The role of estrogens in control of energy balance and glucose homeostasis. *Endocrine Reviews* 34 (3):309–338.
- [4] Rossouw, J.E., Anderson, G.L., Prentice, R.L., LaCroix, A.Z., Kooperberg, C., Stefanick, M.L., et al., 2002. Risks and benefits of estrogen plus progestin in healthy postmenopausal women: principal results from the Women's Health Initiative randomized controlled trial. *Journal of the American Medical Association* 288 (3):321–333.
- [5] Komm, B.S., Kharode, Y.P., Bodine, P.V., Harris, H.A., Miller, C.P., Lyttle, C.R., 2005. Bazedoxifene acetate: a selective estrogen receptor modulator with improved selectivity. *Endocrinology* 146 (9):3999–4008.
- [6] Duggan, S.T., McKeage, K., 2011. Bazedoxifene: a review of its use in the treatment of postmenopausal osteoporosis. *Drugs* 71 (16):2193–2212.
- [7] Komm, B.S., 2008. A new approach to menopausal therapy: the tissue selective estrogen complex. *Reproduction Science* 15 (10):984–992.
- [8] Komm, B.S., Mirkin, S., 2012. Incorporating bazedoxifene/conjugated estrogens into the current paradigm of menopausal therapy. *International Journal of Women's Health* 4:129–140.
- [9] Lobo, R.A., Pinkerton, J.V., Gass, M.L., Dorin, M.H., Ronkin, S., Pickar, J.H., et al., 2009. Evaluation of bazedoxifene/conjugated estrogens for the treatment of menopausal symptoms and effects on metabolic parameters and overall safety profile. *Fertility and Sterility* 92 (3):1025–1038.
- [10] Gruber, C., Gruber, D., 2004. Bazedoxifene (Wyeth). *Current Opinion in Investigational Drugs* 5 (10):1086–1093.
- [11] Komm, B.S., Vlasseros, F., Samadfam, R., Chouinard, L., Smith, S.Y., 2011. Skeletal effects of bazedoxifene paired with conjugated estrogens in ovariectomized rats. *Bone* 49 (3):376–386.
- [12] Lindsay, R., Gallagher, J.C., Kagan, R., Pickar, J.H., Constantine, G., 2009. Efficacy of tissue-selective estrogen complex of bazedoxifene/conjugated estrogens for osteoporosis prevention in at-risk postmenopausal women. *Fertility and Sterility* 92 (3):1045–1052.
- [13] Kharode, Y., Bodine, P.V., Miller, C.P., Lyttle, C.R., Komm, B.S., 2008. The pairing of a selective estrogen receptor modulator, bazedoxifene, with conjugated estrogens as a new paradigm for the treatment of menopausal symptoms and osteoporosis prevention. *Endocrinology* 149 (12):6084–6091.
- [14] Pfizer DOF. Duavee USPI September 2013.
- [15] Rossini, M., Lello, S., Sblendorio, I., Viapiana, O., Fracassi, E., Adami, S., et al., 2013. Profile of bazedoxifene/conjugated estrogens for the treatment of estrogen deficiency symptoms and osteoporosis in women at risk of fracture. *Drug Design, Development and Therapy* 7:601–610.
- [16] Pinkerton, J.V., Pickar, J.H., Racketta, J., Mirkin, S., 2012. Bazedoxifene/conjugated estrogens for menopausal symptom treatment and osteoporosis prevention. *Climacteric* 15 (5):411–418.
- [17] Liu, S., Le May, C., Wong, W.P., Ward, R.D., Clegg, D.J., Marcelli, M., et al., 2009. Importance of extranuclear estrogen receptor- $\alpha$  and membrane G protein-coupled estrogen receptor in pancreatic islet survival. *Diabetes* 58 (10):2292–2302.
- [18] Norris, A.W., Chen, L., Fisher, S.J., Szanto, I., Ristow, M., Jozsi, A.C., et al., 2003. Muscle-specific PPAR $\gamma$ -deficient mice develop increased adiposity and insulin resistance but respond to thiazolidinediones. *Journal of Clinical Investigation* 112 (4):608–618.
- [19] Nohara, K., Waraich, R.S., Liu, S., Ferron, M., Waget, A., Meyers, M.S., et al., 2013. Developmental androgen excess programs sympathetic tone and adipose tissue dysfunction and predisposes to a cardiometabolic syndrome in female mice. *American Journal of Physiology – Endocrinology and Metabolism* 304 (12):E1321–E1330.
- [20] Najjar, S.M., Yang, Y., Fernstrom, M.A., Lee, S.J., Deangelis, A.M., Rjaily, G.A., et al., 2005. Insulin acutely decreases hepatic fatty acid synthase activity. *Cell Metabolism* 2 (1):43–53.
- [21] Tiano, J.P., Delghingaro-Augusto, V., Le May, C., Liu, S., Kaw, M.K., Khuder, S.S., et al., 2011. Estrogen receptor activation reduces lipid synthesis in pancreatic islets and prevents beta cell failure in rodent models of type 2 diabetes. *Journal of Clinical Investigation* 121 (8):3331–3342.
- [22] Kim, J.K., Michael, M.D., Previs, S.F., Peroni, O.D., Mauvais-Jarvis, F., Neschen, S., et al., 2000. Redistribution of substrates to adipose tissue promotes obesity in mice

- with selective insulin resistance in muscle. *Journal of Clinical Investigation* 105 (12):1791–1797.
- [23] Steele, R., 1959. Influences of glucose loading and of injected insulin on hepatic glucose output. *Annals of the New York Academy of Sciences* 82:420–430.
- [24] Homma, H., Kurachi, H., Nishio, Y., Takeda, T., Yamamoto, T., Adachi, K., et al., 2000. Estrogen suppresses transcription of lipoprotein lipase gene. Existence of a unique estrogen response element on the lipoprotein lipase promoter. *Journal of Biological Chemistry* 275 (15):11404–11411.
- [25] Gualillo, O., Gonzalez-Juanatey, J.R., Lago, F., 2007. The emerging role of adipokines as mediators of cardiovascular function: physiologic and clinical perspectives. *Trends in Cardiovascular Medicine* 17 (8):275–283.
- [26] Oda, N., Imamura, S., Fujita, T., Uchida, Y., Inagaki, K., Kakizawa, H., et al., 2008. The ratio of leptin to adiponectin can be used as an index of insulin resistance. *Metabolism* 57 (2):268–273.
- [27] Satoh, N., Naruse, M., Usui, T., Tagami, T., Suganami, T., Yamada, K., et al., 2004. Leptin-to-adiponectin ratio as a potential atherogenic index in obese type 2 diabetic patients. *Diabetes Care* 27 (10):2488–2490.
- [28] Yang, Q., Graham, T.E., Mody, N., Preitner, F., Peroni, O.D., Zabolotny, J.M., et al., 2005. Serum retinol binding protein 4 contributes to insulin resistance in obesity and type 2 diabetes. *Nature* 436 (7049):356–362.
- [29] Zhang, J., Wu, Y., Zhang, Y., Leroith, D., Bernlohr, D.A., Chen, X., 2008. The role of lipocalin 2 in the regulation of inflammation in adipocytes and macrophages. *Molecular Endocrinology* 22 (6):1416–1426.
- [30] Yan, Q.W., Yang, Q., Mody, N., Graham, T.E., Hsu, C.H., Xu, Z., et al., 2007. The adipokine lipocalin 2 is regulated by obesity and promotes insulin resistance. *Diabetes* 56 (10):2533–2540.
- [31] Liu, S., Navarro, G., Mauvais-Jarvis, F., 2010. Androgen excess produces systemic oxidative stress and predisposes to beta-cell failure in female mice. *PLoS One* 5 (6):e11302.
- [32] Volzke, H., Schwarz, S., Baumeister, S.E., Wallaschofski, H., Schwahn, C., Grabe, H.J., et al., 2007. Menopausal status and hepatic steatosis in a general female population. *Gut* 56 (4):594–595.
- [33] Mauvais-Jarvis, P., Vickers CFH, W.J., 1990. *Percutaneous absorption of steroids*. Academic Press Inc., New York.
- [34] Wakil, S.J., 1989. Fatty acid synthase, a proficient multifunctional enzyme. *Biochemistry* 28 (11):4523–4530.
- [35] Kahn, B.B., Alquier, T., Carling, D., Hardie, D.G., 2005. AMP-activated protein kinase: ancient energy gauge provides clues to modern understanding of metabolism. *Cell Metabolism* 1 (1):15–25.
- [36] Zhao, Y., Dunbar, J.D., Kharitonov, A., 2012. FGF21 as a therapeutic reagent. *Advances in Experimental Medicine and Biology* 728:214–228.
- [37] Xu, J., Lloyd, D.J., Hale, C., Stanislaus, S., Chen, M., Sivits, G., et al., 2009. Fibroblast growth factor 21 reverses hepatic steatosis, increases energy expenditure, and improves insulin sensitivity in diet-induced obese mice. *Diabetes* 58 (1):250–259.
- [38] Coskun, T., Bina, H.A., Schneider, M.A., Dunbar, J.D., Hu, C.C., Chen, Y., et al., 2008. Fibroblast growth factor 21 corrects obesity in mice. *Endocrinology* 149 (12):6018–6027.
- [39] Lefebvre, P., Cariou, B., Lien, F., Kuipers, F., Staels, B., 2009. Role of bile acids and bile acid receptors in metabolic regulation. *Physiological Reviews* 89 (1):147–191.
- [40] Rodgers, J.T., Lerin, C., Haas, W., Gygi, S.P., Spiegelman, B.M., Puigserver, P., 2005. Nutrient control of glucose homeostasis through a complex of PGC-1 $\alpha$  and SIRT1. *Nature* 434 (7029):113–118.
- [41] Yonezawa, R., Wada, T., Matsumoto, N., Morita, M., Sawakawa, K., Ishii, Y., et al., 2012. Central versus peripheral impact of estradiol on the impaired glucose metabolism in ovariectomized mice on a high-fat diet. *American Journal of Physiology – Endocrinology and Metabolism* 303 (4):E445–456.
- [42] Cedars, M.I., Judd, H.L., 1987. Nonoral routes of estrogen administration. *Obstetrics and Gynecology Clinics of North America* 14 (1):269–298.
- [43] Arevalo, M.A., Santos-Galindo, M., Lagunas, N., Azcoitia, I., Garcia-Segura, L.M., 2011. Selective estrogen receptor modulators as brain therapeutic agents. *Journal of Molecular Endocrinology* 46 (1):R1–9.
- [44] Purushotham, A., Schug, T.T., Xu, Q., Surapureddi, S., Guo, X., Li, X., 2009. Hepatocyte-specific deletion of SIRT1 alters fatty acid metabolism and results in hepatic steatosis and inflammation. *Cell Metabolism* 9 (4):327–338.
- [45] Aoyama, T., Peters, J.M., Iritani, N., Nakajima, T., Furihata, K., Hashimoto, T., et al., 1998. Altered constitutive expression of fatty acid-metabolizing enzymes in mice lacking the peroxisome proliferator-activated receptor alpha (PPAR-alpha). *Journal of Biological Chemistry* 273 (10):5678–5684.
- [46] Velasco, G., Geelen, M.J., Guzman, M., 1997. Control of hepatic fatty acid oxidation by 5'-AMP-activated protein kinase involves a malonyl-CoA-dependent and a malonyl-CoA-independent mechanism. *Archives of Biochemistry and Biophysics* 337 (2):169–175.
- [47] Ribas, V., Drew, B.G., Soleymani, T., Daraei, P., Hevener, A.L., 2010. Skeletal muscle specific ER $\alpha$  deletion is causal for the metabolic syndrome. *Endocrine Reviews* 31:S5.
- [48] Ribas, V., Nguyen, M.T., Henstridge, D.C., Nguyen, A.K., Beaven, S.W., Watt, M. J., et al., 2010. Impaired oxidative metabolism and inflammation are associated with insulin resistance in ER $\alpha$ -deficient mice. *American Journal of Physiology – Endocrinology and Metabolism* 298 (2):E304–319.
- [49] Najjar, S.M., Boisclair, Y.R., Nabih, Z.T., Philippe, N., Imai, Y., Suzuki, Y., et al., 1996. Cloning and characterization of a functional promoter of the rat pp120 gene, encoding a substrate of the insulin receptor tyrosine kinase. *Journal of Biological Chemistry* 271 (15):8809–8817.
- [50] Pedram, A., Razandi, M., O'Mahony, F., Harvey, H., Harvey, B.J., Levin, E.R., 2013. Estrogen reduces lipid content in the liver exclusively from membrane receptor signaling. *Science Signaling* 6 (276):ra36.
- [51] Tian, J.P., Mauvais-Jarvis, F., 2012. Molecular mechanisms of estrogen receptors' suppression of lipogenesis in pancreatic beta-cells. *Endocrinology* 153 (7):2997–3005.
- [52] Zhu, L., Brown, W.C., Cai, Q., Krust, A., Chambon, P., McGuinness, O.P., et al., 2013. Estrogen treatment after ovariectomy protects against fatty liver and may improve pathway-selective insulin resistance. *Diabetes* 62 (2):424–434.
- [53] Riant, E., Waget, A., Cogo, H., Arnal, J.F., Burcelin, R., Gourdy, P., 2009. Estrogens protect against high-fat diet-induced insulin resistance and glucose intolerance in mice. *Endocrinology* 150 (5):2109–2117.
- [54] Bryzgalova, G., Gao, H., Ahren, B., Zierath, J.R., Galuska, D., Steiler, T.L., et al., 2006. Evidence that oestrogen receptor-alpha plays an important role in the regulation of glucose homeostasis in mice: insulin sensitivity in the liver. *Diabetologia* 49 (3):588–597.
- [55] Pua, J.A., Bailey, C.J., 1985. Effect of ovarian hormones on glucose metabolism in mouse soleus muscle. *Endocrinology* 117 (4):1336–1340.
- [56] Guo, H., Zhang, Y., Brockman, D.A., Hahn, W., Bernlohr, D.A., Chen, X., 2012. Lipocalin 2 deficiency alters estradiol production and estrogen receptor signaling in female mice. *Endocrinology* 153 (3):1183–1193.
- [57] Yang, J., Bielenberg, D.R., Rodig, S.J., Doiron, R., Clifton, M.C., Kung, A.L., et al., 2009. Lipocalin 2 promotes breast cancer progression. *Proceedings of the National Academy of Sciences of the United States of America* 106 (10):3913–3918.
- [58] Shi, H., Gu, Y., Yang, J., Xu, L., Mi, W., Yu, W., 2008. Lipocalin 2 promotes lung metastasis of murine breast cancer cells. *Journal of Experimental and Clinical Cancer Research* 27:83.